A Radio Propagation Model for Wireless Underground Sensor Networks

Suk-Un Yoon, Liang Cheng
Department of Computer Science and Engineering
Lehigh University
Bethlehem, PA, USA
Email: suy309@lehigh.edu, cheng@cse.lehigh.edu

Ehsan Ghazanfari, Sibel Pamukcu, Muhannad T. Suleiman
Department of Civil and Environmental Engineering
Lehigh University
Bethlehem, PA, USA
Email: ehg209@lehigh.edu, sp01@lehigh.edu, mts210@lehigh.edu

***Abstract*—An accurate and simple radio propagation model for underground low-power devices such as wireless sensor nodes is introduced and its performance is evaluated by real wireless sensor nodes. The proposed model describes underground radio signal propagation that is proportional to $e^{-2\alpha\rho}/\rho^2$ where ρ represents the distance and α represents the attenuation constant reflecting the soil properties. To evaluate the proposed underground radio propagation model, experiments measuring the radio signal strength with underground sensor nodes were conducted in various sub-surface conditions. Comparing the theoretical estimations of the underground radio propagation and the measured data, the theoretical model fits the measured data well within a 3.45dBm deviation or with an accuracy of 96.33% on average.**

***Index Terms*—Underground Radio Propagation Model; Wireless Underground Sensor Networks; Measurement of Received Signal Strength.**

I. Introduction

Wireless Sensor Networks (WSNs) have abundant applications for monitoring environmental conditions, such as temperature, light, sound, moisture, motion or pollutants. Wireless Underground Sensor Networks (WUSNs) provide useful information of subsurface environments such as water and mineral content for agriculture, oil leakage from an oil reservoir, or land movement for earthquake monitoring [1]. Spatially distributed underground sensor nodes monitor subsurface conditions and report the information in real-time to the sink or a master node with localized interactions. To deploy a wireless underground sensor network, it is important to understand and model the underground radio propagation between underground sensor nodes. With the underground radio propagation model, network designers can estimate underground communication radius and network capacity. Furthermore, the properties of underground communication medium (i.e. soil) are different from air and the evaluation of the underground radio signal propagation model is required to control the soil properties to verify their effects. But, there is no existing research comparing the underground radio propagation model with measured data from wireless underground sensors.

The main contribution of this paper is that it provides an accurate and simple wireless underground radio propagation model with comparisons to measured data. The paper provides the details of developing the wireless underground radio propagation model which can be used for designing wireless underground sensor networks. The proposed model is generic and is applicable to a wide range of frequencies besides the one used by the current wireless sensors. The proposed underground radio propagation model was evaluated comparing laboratory and field measurements with the data estimated by the theoretical model.

II. Related Works

A. Free-space Propagation

A free-space radio propagation model can be used to predict the Received Signal Strength (RSS) between the transmitter and the receiver based on the clear and unobstructed line-of-sight (LOS) path between them. A well-known radio transmission formula was introduced by H. T. Friis. The received power in free space is given by the Friis free space equation as follows:

$$P_r(d) = \frac{P_t G_t G_r \lambda^2}{(4\pi)^2 d^2 L} \tag{1}$$

where $P_r(d)$ is the received power which is a function of the transmitter-receiver distance, P_t is the transmitted power, G_t is the transmitter antenna gain, G_r is the receiver antenna gain, d is the distance between the transmitter and receiver, L is the system loss factor not related to propagation ($L \geq 1$), and λ is the wavelength [2].

B. Underground Propagation

The radio propagation experiences reflection, diffraction, and scattering over the ground communication as well as in the underground communication. In underground wireless networks, reflection occurs when a propagating electromagnetic wave is confronted by objects such as rocks or the surface between the earth and air. The underground radio propagation is characterized by the soil properties such as the permittivity (ϵ), permeability (μ), and electrical conductivity (σ). For lossy dielectrics, the permittivity and electrical conductivity are dependent on the operating frequency. These two properties characterize the displacement (polarization) current and the conduction current which incur the power losses of the electromagnetic wave in the soil [3]. From these facts, we can infer that the permittivity and electrical conductivity are crucial parameters affecting underground radio propagation.

Researchers have studied a channel model of an underground wireless sensor network using the path loss model [4], [5], [6]. The model is based on the Friis equation and provides an equation describing the received signal strength at a distance d from the transmitter. From the results of the papers, the received signal is described as follows:

$$P_r = P_t + G_r + G_t - [6.4 + 20log(d) + 20log(\beta) + 8.69\alpha d] \quad (2)$$

where P_t is the transmit power, G_r and G_t are the gains of the receiver and transmitter antenna respectively, d is the distance in meters, α is the attenuation constant in $1/m$ and β is the phase shifting constant in $radian/m$. In the theoretical researches [4], [5], [6] trying to provide the characteristics of a wireless channel for underground sensor networks, a correction factor is added to the Friis equation to apply additional path loss in soils. The additional path loss in the equation depends on the attenuation constant α and the phase shifting constant β, which values depend on the dielectric properties of soil. Based on the Peplinski's paper [7], the dielectric properties of soil in the 0.3∼1.3 GHz band were calculated. In the calculation of the path loss, the parameters for underground environments such as operating frequency, the composition of soils, the bulk density, and the volumetric water content are considered. In addition to the attenuation of the radio signal in soil, two channel models, reflection from ground surface and multi-path fading, are introduced based on [2]. But, these models did not provide the comparisons with empirical results and did not address the effects of the soil properties such as the permittivity and electrical conductivity, which are crucial factors on the underground raio propagation. Beside the theoretical approach, there are efforts measuring the underground received signal strength and packet reception ratio with wireless sensor nodes such as MICAz (2.4GHz) and MICA2 (433MHz) including the analysis of soil depth, soil water content, and soil electrical conductivity in [8], [9], [10], [11]. In this paper, an underground radio propagation model approaching from Hertz vector analysis is proposed and its estimations are compared with measurements with the analysis of the effects of the soil properties.

III. An Underground Radio Propagation Model

A. Underground Network Model

Wait and Fuller [12] considers the electromagnetic fields of a vertical electric dipole in a homogeneous conducting half-space using simplifying approximations. Sommerfeld [13] assumes that the Hertz vector of underground radio propagation has only a z component Π, which is referred to as the *potential*. This is conveniently decomposed by writing $\Pi = \Pi^p + \Pi^s$, where Π^p is the primary potential of the source and Π^s is the secondary potential. The latter accounts for the presence of the air interface. Symbols used in the underground radio propagation model are shown in Figure 1. In the underground network model, the underground medium has permittivity $\epsilon = \epsilon_r\epsilon_0$, permeability μ_0, and electrical conductivity σ where ϵ_0 $(8.85\times10^{-12}F/m)$ is the permittivity and μ_0 $(4\pi \times 10^{-7}H/m)$ is the permeability of air.

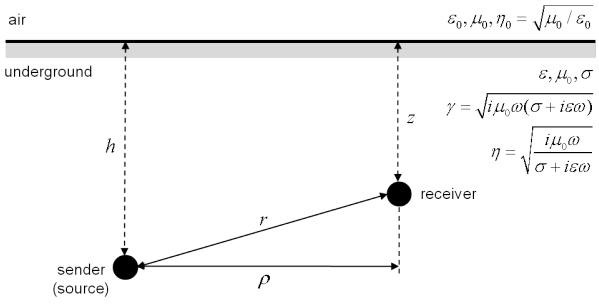

Fig. 1. Symbols used for deriving underground radio propagation model

B. Underground Radio Propagation

In an underground network, a source is imagined to be a vertical electric dipole of length ds and carrying a current I. For a time factor $e^{i\omega t}$ in cylindrical-coordinates, the formal exact expression for the primary potential from a Sommerfeld integral is described as follows:

$$\begin{aligned} \Pi^p &= \frac{Ids}{4\pi(\sigma + i\epsilon\omega)} \frac{e^{-\gamma r}}{r} \\ &= \frac{Ids}{4\pi(\sigma + i\epsilon\omega)} \int_0^\infty \frac{e^{-u|z-h|}}{u} J_0(\lambda\rho)\lambda d\lambda \end{aligned} \quad (3)$$

where ρ is the radial distance from the source, $\gamma = \sqrt{i\mu_0\omega(\sigma + i\epsilon\omega)}$ is the complex propagation constant, $r = \sqrt{\rho^2 + (z-h)^2}$, $u = \sqrt{\lambda^2 + \gamma^2}$, and $J_0(\lambda\rho)$ is the Bessel function of order zero [12]. The integration variable λ can be identified with the sine of a plane wave spectrum of complex angle θ via $\lambda = -i\gamma \sin\theta$. The secondary potential underground is described as follows:

$$\Pi^s = \frac{Ids}{4\pi(\sigma + i\epsilon\omega)} \int_0^\infty \frac{e^{-u(z+h)}}{u} R(\lambda) J_0(\lambda\rho)\lambda d\lambda \quad (4)$$

where $R(\lambda) = \frac{u - Ku_0}{u + Ku_0}$ is a Fresnel reflection factor, $u_0 = \sqrt{\lambda^2 + \gamma_0^2}$, $\gamma_0 = i\omega\sqrt{\epsilon_0\mu_0}$, and $K = \frac{\sigma + i\epsilon\omega}{i\epsilon_0\omega}$ [12].

The vertical electric-field component, E_z, at the receiver is the observable quantity from the primary and secondary potentials as follows:

$$\begin{aligned} E_z &= E_z^p + E_z^s = \left(-\gamma^2 + \frac{\partial^2}{\partial z^2}\right)[\Pi^p + \Pi^s] \\ &= \frac{Ids}{4\pi(\sigma + i\epsilon\omega)\rho^3}(C^p + C^s) \end{aligned} \quad (5)$$

where

$$C^p = \left(-\Gamma^2 + \frac{\partial^2}{\partial D_0^2}\right)\left[\frac{e^{-\Gamma\Re}}{\Re}\right], \quad (6)$$

and

$$C^s = \int_0^\infty \frac{e^{-UD}}{U} R(x) J_0(x) x^3 dx \quad (7)$$

where C^p and C^s are the primary and secondary contributions, $\Gamma = \gamma\rho$, $D_0 = \frac{|z-h|}{\rho}$, $\Re = \sqrt{D_0^2 + 1}$, $x = \lambda\rho$ is the integration variable, $U = \sqrt{x^2 + \Gamma^2}$, $D = \frac{z+h}{\rho}$, $R(x) = \frac{U - KU_0}{U + KU_0}$, and

$U_0 = \sqrt{x^2 - (\frac{\omega\rho}{c})^2}$ [12]. After the mathematical calculations, the result of the primary contribution is described as follows:

$$C^p = e^{-\gamma r}\left(\frac{\rho}{r}\right)^3\{-1-\gamma r(1+\gamma r) + \left[1-\left(\frac{\rho}{r}\right)^2\right]\left[3(1+\gamma r)+(\gamma r)^2\right]\}. \quad (8)$$

The secondary contribution C^s could be neglected if the air interface was sufficiently removed from the source and observer locations (i.e., deep burial depths). If $z = h$ (the same depth for the sender and receiver) and the burial depth is deep enough, the electric-field can be simplified as follows:

$$E_z = \frac{Ids}{4\pi(\sigma+i\epsilon\omega)\rho^3}\{-e^{-\gamma\rho}\left[1+\gamma\rho+(\gamma\rho)^2\right]\}. \quad (9)$$

With the radiating electric-field component, the received signal power in $Watts$ can be calculated as follows:

$$P_r = A_{eff}\frac{|E_z|^2}{2|\eta|}cos\theta_\eta \quad (10)$$

where A_{eff} is the effective antenna area of the receiver, $\eta = \sqrt{\frac{i\mu\omega}{\sigma+i\epsilon\omega}}$ is the intrinsic wave impedance of the medium, and θ_η is the phase angle of the intrinsic impedance $\eta = |\eta|e^{j\theta_\eta}$. For a thin linear half-wave antenna in a wireless sensor network, the effective antenna area is determined by the wavelength as follows: A_{eff}=$\frac{\lambda}{2}(0.26\lambda)$ [3]. The result of the received signal of the wireless underground sensor node with a whip antenna is expressed as follows:

$$P_r = \frac{0.26\lambda^2 cos\theta_\eta}{4|\eta|}\left|\frac{Ids\{-e^{-\gamma\rho}[1+\gamma\rho+(\gamma\rho)^2]\}}{4\pi(\sigma+i\epsilon\omega)\rho^3}\right|^2. \quad (11)$$

If $|\gamma\rho| \gg 1$, the received signal strength at distance ρ can be simplified as follows:

$$\begin{aligned} P_r(\rho) &\simeq \frac{A_{eff}cos\theta_\eta}{2|\eta|}\left|\frac{-Ids\times i\mu_0\omega e^{-\gamma\rho}}{4\pi\rho}\right|^2 \\ &= K\left|\frac{e^{-\gamma\rho}}{\rho}\right|^2 = K\left|\frac{e^{-2\gamma\rho}}{\rho^2}\right| \\ &= K\frac{e^{-2\alpha\rho}}{\rho^2} \end{aligned} \quad (12)$$

where $K = \frac{A_{eff}cos\theta_\eta}{2|\eta|}(\frac{Ids\mu_0\omega}{4\pi})^2$ is a constant and $\alpha = Re(\gamma) = \omega\sqrt{\frac{\mu\epsilon}{2}\left[\sqrt{1+\left(\frac{\sigma}{\omega\epsilon}\right)^2}-1\right]}$ is the attenuation constant of the medium.

The received signal of the wireless underground sensors is proportional to $e^{-2\alpha\rho}/\rho^2$ where ρ represents the distance between the sender and the receiver and α represents the attenuation constant which is determined by the soil properties such as permittivity and electric conductivity. In the simplification a condition, $|\gamma\rho| \gg 1$, is required. To verify the condition, the $|\gamma\rho|$ is calculated in the frequency ranges of sensor networks including 2.4GHz (MICAz) and 400MHz (MICA2) and the values of $|\gamma\rho|$ are greater than 1 at different distances including close distances. The detail data and figures data are shown in [14].

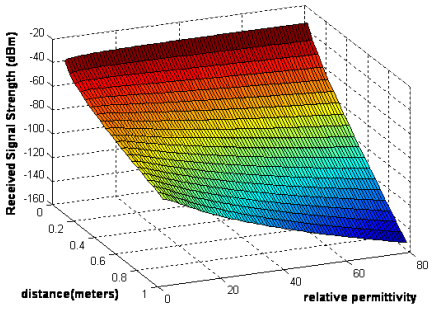

Fig. 2. RSS with relative permittivity (ϵ_r) of soil and distance (ρ)

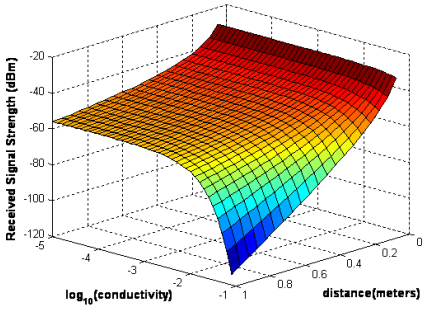

Fig. 3. RSS with electric conductivity (σ) of soil and distance (ρ)

The underground received signal in the proposed equation experiences signal attenuations depending on the underground medium's properties, which are permittivity and electric conductivity. To evaluate the effect of permittivity, we calculated and plotted the received signal strength of 2.4 GHz sensor nodes with respect to distance in Figure 2. The maximum communication distance of the underground sensor network is expected less than 1 meter in 2.4 GHz [8], [9], we chose the short distance of 0.05$\sim$1 meters in the calculation. The range of relative permittivity (ϵ_r) is 2$\sim$79 (ex, 1: air, 80: water) with a loss tangent ($tan\delta$=ϵ''/ϵ'=0.05, estimated from [7]) where ϵ=$\epsilon' - i\epsilon''$. In Figure 2, the received signal strength decreases as the relative permittivity increases in the permittivity range of soils (relative permittivity of saturated sandy soil: 19$\sim$30 [15]).

To investigate the effect of electric conductivity, we calculated the received signal strength in the distance of 0.05$\sim$1 meters with the relative permittivity of 20 in Figure 3. The range of electric conductivity is $10^{-1}\sim10^{-5}$ (ex, electric conductivity of drinking water: 0.0005$\sim$0.05, electric conductivity of soil: $\sim10^{-1}$ [16]). In Figure 3, the received signal strength dramatically changes in the range of conductivity between 10^{-1} and $10^{-2.5}$ S/m. Increasing the distance in the range of electric conductivity between 10^{-1} and $10^{-2.5}$ S/m causes the signal strength to decay quickly due to high attenuations in the soil. Because the transmission power is set to be 0dBm in the comparisons, the received signal strength converges to

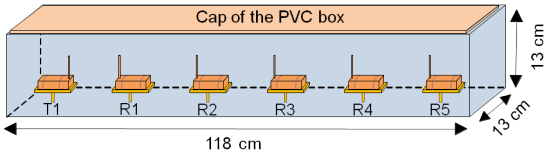

(a) Designed PVC box to install sensors (one transmitter and five receivers)

(b) PVC box with sensors before soil filling

(c) Installed sensors in the box with temperature probes before burying

Fig. 4. Details of laboratory and field test preparation

Tx power level (0dBm) as the distance goes to 0. With the proposed underground radio propagation model, the received power can be expressed by a log scale model as follows:

$$\left[\frac{P_r(\rho)}{P_r(\rho_0)}\right]_{dB} \simeq 10log\left[\left(\frac{\rho_0}{\rho}\right)^2 e^{-2\alpha(\rho-\rho_0)}\right] = -20log\left(\frac{\rho}{\rho_0}\right) - 8.6859\alpha(\rho-\rho_0) \quad (13)$$

where ρ_0 is the close-in reference distance which is close to the transmitter, and ρ is the transmitter-receiver distance. The log scale expression has a similar form to the log-normal shadowing model with a pass loss exponent n=2 and an additional path loss term instead of a shadowing deviation. The logarithmic expression is consistent with the result form of equation 2 reported in [4], [5], [6], even though the derivation methods are different.

IV. Performance Evaluations

To evaluate the accuracy of the proposed underground radio propagation model, various experiments in the laboratory and in the field were conducted using MICAz. All wireless sensor nodes are calibrated and selected to be working in 1∼2 dBm error bounds on the received signal strength measurement. As an underground medium, two types of sand were used: uniform size construction sand (D_{10}=0.2mm, D_{30}=0.34mm, and D_{60}=0.67mm) and uniform size sandblast (D_{10}=0.40mm, D_{30}=0.51mm, and D_{60}=0.62mm) where D_x is the diameter of the soil particles for which $x\%$ of the particles are finer.

A. Experimental conditions

1) Laboratory tests: To control the soil properties, a small plastic (PVC) box with dimensions 118×13×13cm was made and the sensors are installed in the box as shown in Figure 4(a) and 4(b). In each experiment, the soil properties (water content (the ratio of water volume in total volume), saturation, salinity, compaction, and soil gradation) and physical properties of the environment such as temperature, which affects the electric conductivity and permittivity of the medium, were controlled.

2) Field test: The field tests were conducted at a remote corner of the athletic field facilities of Lehigh University. This area was selected because of its isolation from existing Wi-Fi interference and surface noise, distance from major underground facilities, and type of the sandy soil encountered which matched reasonably well with the sand used in laboratory experiments. The field tests were conducted at the burial depth of 140cm for thermal and moisture isolation as well as isolation from EM interferences. A square trench of 150×150cm was excavated to 140cm depth using a backhoe. The small test box underground was also equipped with two thermocouples underneath the top cap to monitor the temperature of the test sand as shown in Figure 4(c). The field tests were conducted for the duration of 4 days, during which the sensors sampled the received signal strength and stored the data on the flash memory at 15 second intervals.

B. Comparison of results

The received signal strengths with 0dBm Tx power in the laboratory and field tests were measured for 8%, 12%, and 15% wet sand and compared with the theoretical received signal strength estimation using Equation 12 and the measured electric conductivity (shown in [14]) of the sand based on ASTM (American Society for Testing and Materials) G187 standard [17]. In the comparisons, the average absolute deviation (D in dBm scale) between the theoretical estimations and the measured data on N positions is calculated as follows: $D = \frac{1}{N}\sum_{i=1}^{N}|P^i_{estimated} - P^i_{measured}|$. Then, the accuracy ($A$, %) based on the Tx power (P_t) and minimum sensible power (P_{min} = −94dBm [9]) in the dBm scale were calculated as follows: $A = [1 - \frac{D}{|P_t - P_{min}|}] \times 100$. The permittivity of the wet sand was used from estimated values in the range of ϵ_r=19∼30. The theoretical estimation (σ=86.96mS/m, ϵ_r=19), laboratory measurements, and field measurements for the 12% wet sand with 5000ppm salinity are compared in Figure 5(a). The average deviation between the laboratory and field measurements was 5.2dBm which was the amount of deviation seen in different laboratory experiments.

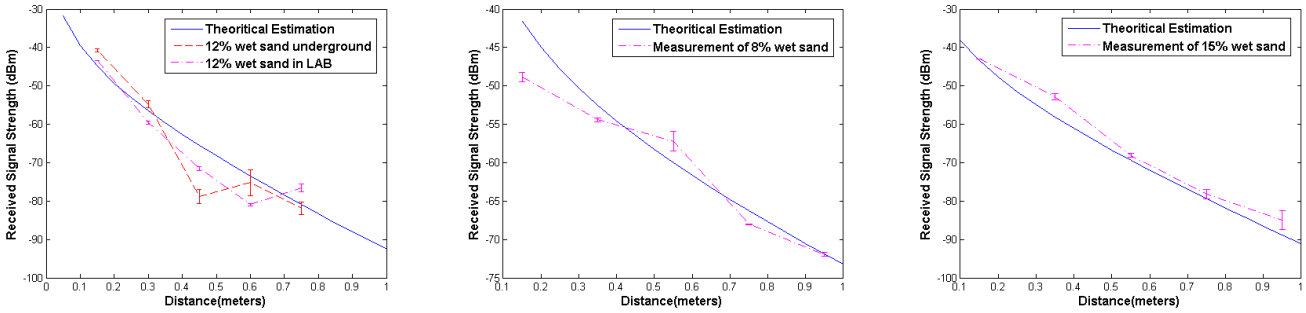

(a) 12% wet sand with salinity (5000ppm); theoretical estimation vs. field and laboratory measurements

(b) 8% wet sand with salinity (5000ppm); theoretical estimations vs. laboratory measurements

(c) 15% wet sand with salinity (1000ppm); theoretical estimations vs. laboratory measurements

Fig. 5. Comparisons of theoretical estimations and measured data

The average deviation and accuracy between the theoretical estimation and the field measurement were 4.36dBm and 95.36% respectively, and the average deviation and accuracy between the estimation and the laboratory measurement were 4.49dBm and 95.22% respectively. The theoretical estimations (8% wet sand: σ=37.61mS/m, ϵ_r=19; 15% wet sand: σ=123.61mS/m, ϵ_r=30), laboratory measurements for the 8% wet sand with 5000ppm salinity and 15% wet sand with 1000ppm salinity are compared in Figure 5(b) and 5(c). The average deviation and accuracy between the theoretical estimation and the 8% wet sand measurement were 3.19dBm and 96.6% respectively, and the average deviation and error between the estimation and the 15% wet sand measurement were 1.77dBm and 98.11%, respectively. In the comparisons, the theoretical received signal strength estimation fits the measured data well within a 3.45dBm deviation or with an accuracy of 96.33% on average.

V. Conclusion

The paper provides theories and measured results to improve the understanding of the radio signal propagation of wireless underground sensor networks. Based on the theories, we developed the received signal and path loss models of the underground sensor nodes with respect to the distance between the sender and the receiver. The proposed model was validated using laboratory and field measurements. The estimated received signal strength from the underground radio propagation model provides a very good fit to the measured data of the wireless underground sensor network.

Acknowledgment

This material is based upon work partly supported by the National Science Foundation (NSF) under Grant No. 0855603. Any opinions, findings, and conclusions or recommendations expressed in this material are those of the author(s) and do not necessarily reflect the views of the NSF.

References

[1] Ian F. Akyildiz, Erich P. Stuntebeck, Wireless underground sensor networks: Research challenges, Ad Hoc Networks Journal (Elsevier), Vol. 4, No. 6, pp. 669-686, November 2006.

[2] T. S. Rappaport, Wireless communications Principles and Practice, Prentice Hall, 1996.

[3] Sophocles J. Orfanidis, Electromagnetic Waves and Antennas, Online Book. http://www.ece.rutgers.edu/~orfanidi/ewa

[4] L. Li, M.C. Vuran, I.F. Akyildiz, Characteristics of underground channel for wireless underground sensor networks, Proc. IFIP Mediterranean Ad Hoc Networking Workshop, Corfu, Greece, June 2007.

[5] M. C. Vuran and I. F. Akyildiz, Channel Model and Analysis for Wireless Underground Sensor Networks in Soil Medium, Physical Communication Journal (Elsevier), 2010.

[6] I. F. Akyildiz, Z. Sun, M. C. Vuran, Signal Propagation Techniques for Wireless Underground Communication Networks, Physical Communication Journal (Elsevier), vol. 2, no. 3, pp. 167-183, Sept. 2009.

[7] Neil R. Peplinski, Fawwaz T. Ulaby, and Myron C. Dobson, Dielectric Properties of Soils in the 0.3-1.3-GHz Range, IEEE Transactions On Geoscience and Remote Sensing, VOL. 33, NO. 3, May 1995.

[8] A. R. Silva and M. C. Vuran, Empirical evaluation of wireless underground-to-underground communication in wireless underground sensor networks, IEEE DCOSS '09, Marina Del Rey, CA, June 2009.

[9] E. Stuntebeck, D. Pompili, T. Melodia, Underground Wireless Sensor Networks Using Commodity Terrestrial Motes, Poster presentation at IEEE SECON 2006, September 2006.

[10] Ehsan Ghazanfari, Suk-Un Yoon, Yi Dong, Xu (Eric) Li, Carlos I. Medina, Donald Seserko, Liang Cheng, Tae Sup Yun, Sibel Pamukcu, Subsurface geo-event monitoring using wireless sensor networks, Geo-Frontiers Conference 2011, March 2011.

[11] Bogena H. R., Huisman J. A., Meier H., Rosenbaum U., Weuthen A., Hybrid Wireless Underground Sensor Networks: Qualification of Signal Attenuation in Soil, Vadose Zone Journal Vol. 8 No. 3 pp. 755-761, 2009.

[12] Jams R. WAIT and Jams A. FULLER, On Radio Propagation through Earth, IEEE Transactions On Antennas and Propagation, Nov. 1971.

[13] A. Sommerfeld, ber die ausbreitung der wellen in der drahtlosen telegraphie, Ann. Phys. Lpz., 28, 665-736, 1909.

[14] Suk-Un Yoon, Liang Cheng, Ehsan Ghazanfari, Sibel Pamukcu, and Muhannad T. Suleiman, An Underground Radio Propagation Model for Wireless Underground Sensor Networks, Technical Reports LU-CSE-10-007, 2010. http://www3.lehigh.edu/images/userImages/jgs2/Page_7287/LU-CSE-10-007.pdf

[15] Hubbard, S. S., J. E. Peterson, Jr., E. L. Majer, P. T. Zawislanski, K. H. Williams, J. Roberts, and F. Wobber, Estimation of permeable pathways and water content using tomographic radar data, The Leading Edge, 16, 1623-1628, 1997.

[16] K. Rohini and Devendra N. Singh, Methodology for Determination of Electrical Properties of Soils, Journal of Testing and Evaluation, Vol. 32, No. 1, Jan. 2004.

[17] ASTM, Standard Test Method for Measurement of Soil Resistivity Using the Two-Electrode Soil Box Method, Designation: G187-05.